Mapping the Differential Distribution of Glycosaminoglycans in the Adult Human Retina, Choroid, and Sclera

Simon J. Clark,[1,2] *Tiarnan D. L. Keenan,*[2,3,4] *Helen L. Fielder,*[1,2,5] *Lisa J. Collinson,*[1] *Rebecca J. Holley,*[6] *Catherine L. R. Merry,*[6] *Toin H. van Kuppevelt,*[7] *Anthony J. Day,*[*,1] *and Paul N. Bishop*[*,3,4]

Purpose. To map the distribution of different classes of glycosaminoglycans (GAGs) in the healthy human retina, choroid, and sclera.

Methods. Frozen tissue sections were made from adult human donor eyes. The GAG chains of proteoglycans (PGs) were detected with antibodies directed against various GAG structures (either directly or after pretreatment with GAG-degrading enzymes); hyaluronan (HA) was detected using biotinylated recombinant G1-domain of human versican. The primary detection reagents were identified with FITC-labeled probes and analyzed by fluorescence microscopy.

Results. Heparan sulfate (HS), chondroitin sulfate (CS), dermatan sulfate (DS), and HA were present throughout the retina and choroid, but keratan sulfate (KS) was detected only in the sclera. HS labeling was particularly strong in basement membrane–containing structures, the nerve fiber layer (NFL), and retinal pigment epithelium (RPE)—for example, intense staining was seen with an antibody that binds strongly to sequences containing 3-*O*-sulfation in the internal limiting membrane (ILM) and in the basement membrane of blood vessels. Unsulfated CS was seen throughout the retina, particularly in the ILM and interphotoreceptor matrix (IPM) with 6-*O*-sulfated CS also prominent in the IPM. There was labeling for DS throughout the retina and choroid, especially in the NFL, ganglion cell layer, and blood vessels.

Conclusions. The detection of GAG chains with specific probes and fluorescence microscopy provides for the first time a detailed analysis of their compartmentalization in the human retina, by both GAG chain type and sulfation pattern. This reference map provides a basis for understanding the functional regulation of GAG-binding proteins in health and disease processes. (*Invest Ophthalmol Vis Sci.* 2011;52:6511–6521) DOI:10.1167/iovs.11-7909

From the [1]Wellcome Trust Centre for Cell-Matrix Research, Faculty of Life Sciences, the [3]School of Biomedicine, and the [6]Materials Science Centre, University of Manchester, Manchester, United Kingdom; the [4]Manchester Academic Health Sciences Centre, Royal Eye Hospital, Central Manchester University Hospitals NHS Foundation Trust, Manchester, United Kingdom; the [5]Department of Biochemistry, University of Oxford, Oxford, United Kingdom; and the [7]Department of Biochemistry, Radboud University Nijmegen Medical Center, Nijmegen, The Netherlands.

[2]These authors contributed equally to the work presented here and should therefore be regarded as equivalent authors.

Supported by Macular Disease Society, Medical Research Council Grant G0900592, Arthritis Research UK Grant 18472, and the Manchester NIHR Biomedical Research Centre. The Bioimaging Facility microscopes used in this report were purchased with grants from the BBSRC (Biotechnology and Biological Sciences Research Council), Wellcome Trust, and the University of Manchester Strategic Fund. TDLK is a recipient of a Fight for Sight Clinical Fellowship (1866) and HLF was funded by an MRC Studentship. The unlabelled and biotinylated VG1 described in this report are commercially available through COSMO Bio Co. Ltd., Japan. AJD receives royalties on the sale of these reagents.

Submitted for publication May 19, 2011; revised June 23, 2011; accepted June 23, 2011.

Disclosure: **S.J. Clark**, None; **T.D.L. Keenan**, None; **H.L. Fielder**, None; **L.J. Collinson**, None; **R.J. Holley**, None; **C.L.R. Merry**, None; **T.H. van Kuppevelt**, None; **A.J. Day**, P; **P.N. Bishop**, None

*Each of the following is a corresponding author: Paul N. Bishop, School of Biomedicine, AV Hill Building, University of Manchester, Oxford Road, Manchester M13 9PT, UK;
paul.bishop@manchester.ac.uk.
Anthony J. Day, Faculty of Life Sciences, Michael Smith Building, University of Manchester, Oxford Road, Manchester M13 9PT, UK;
anthony.day@manchester.ac.uk.

Proteoglycans (PGs) are present on cell surfaces and are a major component of the extracellular matrix, where they have key roles in regulating multiple physiological and pathologic processes[1–3]; PGs are composed of a core protein with one or more glycosaminoglycan (GAG) chains attached. GAG chains are long, unbranched polysaccharides composed of repeating disaccharide units differing from one another in their disaccharide composition, linkages, and levels of sulfation.[4] Based on their GAG chain composition, PGs are classified into four families: heparan sulfate (HS), chondroitin sulfate (CS), dermatan sulfate (DS), and keratan sulfate (KS). There are two further GAGs present in vertebrates: heparin and hyaluronan (HA). Heparin, produced by mast cells, is a highly sulfated version of HS that is made as a PG and then secreted in a largely protein-free form.[5] Hyaluronan, which is widely expressed in tissues,[6,7] is completely unsulfated and is the only mammalian GAG that is not synthesized in association with a core protein.

Previously, PGs have been extracted from the extracellular matrices, basal lamina, and cell membranes of developing eyes of rat, mouse, and zebrafish, and certain PGs have also been identified directly in human eyes by using various staining methods.[8] However, there has been no detailed analysis of the distribution of GAGs in the adult human retina. Given the importance of GAG chain type and sulfation pattern in defining the specificity of protein binding,[4,9] a detailed understanding of their localization in the retina will provide novel insights into their functions. In this study, we compiled a map of GAGs in the human adult retina, choroid, and sclera by using fluorescence microscopy and demonstrated that GAGs are more widely distributed than previous studies imply and that specific sulfation patterns are differentially distributed between various tissue layers.

METHODS

Tissue Section Preparation

Eyes were obtained from the Manchester Royal Eye Hospital Eye Bank after removal of the corneas for transplantation. Each experiment reported in this study was performed separately on tissue sections of eyes from three adult donors (males aged 59 and 81 years; a female age 82 years). Our research adhered to the tenets of the Declaration of Helsinki. In all cases, there was prior consent for the eye tissue to be used for research, and guidelines established in the Human Tissue Act of 2004 (U.K.) were followed. None of the donors had a history of visual impairment or eye disease.

Donor eyes were fixed within 24 hours after death in 4% (vol/vol) formaldehyde for 2 hours at room temperature, essentially as described previously.[10] Briefly, the macular region was removed with a 5-mm diameter biopsy punch (Schüco International, Kingston Milton Keynes, UK), centered on the fovea, and further fixed in 4% (vol/vol) formaldehyde for 16 hours at 4°C. Each sample was set in OCT cryoprotectant (RA Lamb, Eastbourne, UK); 5-μm tissue slices were made with a cryostat (CM1850; Leica, Wetzlar, Germany) and mounted on poly-L-lysine-coated microscope slides (Menzel-Gläser, Saarbrückene, Germany). If the slides were not used immediately, they were stored at −80°C. The length of time each tissue sample was stored at −80°C did not affect the staining pattern observed with any of the detection reagents used in this study.

Tissue Pretreatment and GAG-Chain Staining

Staining protocols were performed for all sulfated GAG classes by applying the appropriate combination of enzymatic pretreatment (where required) and antibody, as listed in Table 1.

Before staining and tissue pretreatments, the microscope slides were incubated with chilled (−20°C) histologic grade acetone (Sigma-Aldrich, Poole, UK) for 20 seconds before they were thoroughly washed in PBS (137 mM NaCl, 2.6 mM KCl, 8.2 mM Na_2HPO_4, and 1.5 mM KH_2PO_4 [pH 7.3]; Oxoid, Basingstoke, UK). Squares were drawn around each tissue section with a hydrophobic barrier pen (Vector Labs, Peterborough, UK), to prevent contamination from treatments used on adjacent samples.

Enzymatic pretreatments, where required, were performed as described previously in Clark et al.[10] Briefly, 20 U/mL enzyme (i.e., chondroitin AC lyase, chondroitin B lyase, or heparinase I/II/III mix; all from *Flavobacterium heparinum*) or 50 U/mL hyaluronidase (from *Streptomyces hyalurolyticus*) were used in PBS at 37°C for 1 hour (all enzymes purchased from Sigma-Aldrich). Tissue was blocked by incubation with 100 μL/section blocking buffer (PBS, 1 mg/mL BSA, 1% [wt/vol] goat serum, and 0.1% [vol/vol] Triton X-100) at 37°C for 1 hour. Control experiments were also conducted in which tissue sections were treated with blocking buffer without enzyme. In the case of VSVg-tagged anti-HS antibodies (AO4B08, RB4EA-12, LKIV69, and HS4C3),[12–15,23,24] the pan-HS antibody 10E4,[11] and the anti-whole-chain C4S antibody LY111 (Seikagaku Corporation, Tokyo, Japan),[17] each was diluted 1:20 with blocking buffer before application to tissue sections (100 μL/section) and incubated for 16 hours at 4°C. After extensive washing of the tissue with PBS, the AlexaFluor 488-conjugated secondary antibody (i.e., rabbit anti-VSVg for the VSVg-tagged antibodies, or goat anti-rabbit [all from Molecular Probes, Paisley, UK] for the 10E4 or LY111 antibodies) diluted 1:200 with PBS, was added to each tissue section for 2 hours at room temperature.

In addition to the anti-CS antibody described above that binds to internal regions within whole GAG chains, detection of CS and DS was also performed with anti-stub antibodies (1B5, 2B6, and 3B3; MD Biosciences, Zurich, Switzerland) that recognize these GAGs only after their digestion with specific enzymes (i.e., chondroitin AC lyase or chondroitin B lyase, respectively).[16] Staining with these antibodies was performed as described above, but the primary antibodies were diluted 1:100 and the secondary antibody (AlexaFluor 488-conjugated goat anti-mouse IgG; Molecular Probes, Paisley, UK) was diluted 1:250.

TABLE 1. List of Antibodies Used for Labeling Specific Sulfated GAGs, Together with Characteristics of Antibody Epitope on the GAG Chain, Enzymes Applied to Tissues before Antibody Treatment, and Associated References

	Heparan Sulfate					Chondroitin Sulfate				Dermatan Sulfate	Keratan Sulfate
Antibody	10E4	LKIV69*	RB4EA-12*	AO4B08*	HS4C3*	1B5	3B3	2B6	LY111	2B6	5D4
Principle epitopes	Pan-HS	N- and 2-*O* sulfation	N- and 6-*O* sulfated disaccharide units	N- and 6-*O* sulfated octa-saccharide with internal 2-*O* sulfate	3-*O* sulfate containing Hexa- to Octa-saccharide	Unsulfated stubs	C-6-sulfated stubs	C-4-sulfated stubs	Whole-chain C4S	DS stubs	Pan-KS
Binding inhibited	—	6-*O* sulfation	2-*O* sulfation	—	—	—	—	—	—	—	—
Enzyme used for tissue pretreatment	—					Chondroitin AC lyase			—	Chondroitin B lyase	—
Reference	11	12	13	14	15		16		17	18	19

* The specificities of the phage-display antibodies described here were determined by direct binding to defined oligosaccharides; additional analysis using naturally occurring HS chains (e.g. on stem cell surfaces) has provided further information on the range and hierarchy of GAG structures recognized.[20–22]

Staining of untreated eye tissue, where GAGs were not digested, acted as a control for the specificity of the antibodies.

Hyaluronan was stained with either bVG1 (expressed, purified, and biotinylated as described in detail below) or biotinylated bovine nasal cartilage–derived hyaluronan-binding protein (bHABP; Seikagaku) at 10 μg/mL in blocking buffer for 16 hours at 4°C. The bound biotinylated proteins were detected with AlexaFluor 488-conjugated streptavidin (Molecular Probes) diluted 1:500 in PBS.

Image Capture and Data Analysis

Images were collected on an upright microscope (model BX51; Olympus, Tokyo, Japan), with a 20×/0.30 Plan Fln objective and captured with a digital camera (Coolsnap ES; Photometrics, Maidenhead, UK, with MetaVue Software ver. 6.1; Molecular Devices, Sunnyvale, CA), essentially as described previously.[10] Specific band-pass filter sets for DAPI and FITC were used to prevent bleedthrough from one channel to the next. Images were then processed and analyzed using ImageJ64 (ver. 1.40g; developed by Wayne Rasband, National Institutes of Health, Bethesda, MD; available at http://rsb.info.nih.gov/ij).

For the three-dimensional modeling of retinal blood vessels, 451 *z*-section images (0.01-μm separation) were taken using a confocal microscope (C1Eclipse; Nikon, Tokyo, Japan) mounted on an upright microscope with a 40×/0.75 Plan Fluor objective and the following settings: pinhole, 30 μm; scan speed, 400 Hz unidirectional; format, 1024 × 1024. Data were processed using 3D viewer function in ImageJ64.

Analysis of the staining results from all three donors was performed independently by SJC and TDLK. Both graders were blinded to the experimental conditions and applied previously agreed scoring criteria to determine the level of staining present in each tissue layer. Their independent scoring tables were merged to produce the final experimental analysis (Table 2).

HA-Detection Reagent: Expression, Purification, and Biotinylation of VG1

The VG1 coding sequence, nucleotides 327-1316,[25] was amplified by PCR from a pMT/V5-His vector containing the cDNA previously used to express VG1 in *Drosophila* S2 cells[26] and cloned into pRK172. The new construct was transformed into *Escherichia coli* BL21(DE3)pLysS cells (Novagen, Nottingham, UK), which were grown to an OD_{600nm} value of 0.4 in Luria broth (containing 34 μg/mL chloramphenicol and 100 μg/mL ampicillin) at 37°C with shaking (~150 rpm), induced with 1 mM IPTG (final concentration), grown for a further 20 hours, and harvested by centrifugation (20 minutes, 1600*g*). Inclusion bodies were purified[27] and solubilized in urea and the protein refolded, essentially as described previously.[28,29] Briefly, inclusion bodies were solubilized in 8 M urea, 1 mM EDTA, 0.1 M Tris, 25 mM DTT (pH 8.0, adjusted to pH 3 to 4 with HCl) and clarified by centrifugation. The supernatant was dialyzed into 6 M urea and 10 mM HCl, and the protein concentration was adjusted to 2 mg/mL with the dialysis buffer and then diluted 66-fold into 1 mM EDTA, 0.5 M L-arginine, 1 mM cysteine, 2 mM cystine, and 0.02 M ethanolamine (pH 11.0) by dropwise addition at 4°C with gentle stirring, followed by incubation for 18 hours without stirring. After refolding, the protein was concentrated to 150–200 mL in a crossflow ultrafiltration unit (Vivaflow 200 blocks; 5-kDa molecular weight cutoff, PES membrane; Vivascience, Surrey, UK), dialyzed overnight into 50 mM Tris, 150 mM NaCl, and 1 mM EDTA (pH 8.5), and purified on a 47 × 26-mm column (25 mL; Q Sepharose Fast Flow column; GE Healthcare, Amersham, UK) equilibrated in 50 mM Tris, 150 mM NaCl, 1 mM EDTA (pH 8.5). The recombinant VG1 was then eluted with 0% to 30% 50 mM Tris, 1 M NaCl, 1 mM EDTA (pH 8.5) in equilibration buffer over 4.2 column volumes at 3 mL/min. Fractions containing VG1 and found to be essentially free of contaminating proteins, as determined by SDS-PAGE (under reducing conditions), were pooled and dialyzed into PBS. The protein concentration was determined based on the A_{280nm} of a 1 mg/mL solution = 1.27, which was calculated from the VG1 amino acid composition.

The HA-binding activity of VG1 was verified using a microtiter plate–based assay described previously.[26] VG1 was immobilized (0–11 pmol/well) on ELISA plates (Maxisorp F96; Nunc, Roskilde, Denmark) and binding was assessed with 12.5 ng/well biotinylated-HA in 50 mM HEPES, 100 mM NaCl, and 0.05% (vol/vol) Tween 20, (pH 7.4), where the absorbance at 405 nm was determined after a 15-minute development and corrected by subtracting values from the uncoated wells.

Preparation of biotinylated VG1 (bVG1) was performed as described previously (for the *Drosophila* expressed VG1 protein) in Kuznetsova et al.[30] Briefly, VG1 (2.5 mL, ~70 μg/mL) was added to 432 μL of 5 mg/mL HA (Hylumed Medical grade; Genzyme, Oxford, UK) in water and incubated for 1 hour to saturate HA-binding sites. To this, bovine testicular hyaluronidase (Calbiochem, Nottingham, UK; 48 μL at 7000 units/mL PBS) was added, and the mixture was incubated at 37°C for 1 hour. NHS-LC biotin (0.44 mg; Pierce, Loughborough, UK) was dissolved in DMSO (95.7 μL) and diluted to a final concentration of 0.22 mg/mL in 100 mM $NaHCO_3$ (pH 8.5; 2 mL final volume). This biotin solution was added to the VG1 and rotated at room temperature for 1 hour. The resulting bVG1 was immediately purified by reversed-phase HPLC and lyophilized, as described for unmodified VG1.[26]

Results

Distribution of HS

The 10E4 antibody recognizes a common *N*-sulfated epitope within HS[11] and therefore allows the determination of the overall distribution of HS in the retina. From Figure 1, it can be seen that HS was present in all layers of the retina and in the choroid. There was strong labeling with the HS antibodies of basement membrane–containing structures—that is, the ILM, blood vessels and Bruch's membrane; these are known to contain HSPGs such as perlecan, agrin, and type XVIII collagen.[31,32] However, with this and other data presented on inner limiting membrane (ILM) staining, it was not possible to rule out a contribution from cortical vitreous gel contained within the ILM. In addition, pronounced staining with HS antibodies was observed in the nerve fiber layer (NFL), ganglion cell layer (GCL), and RPE. Detection was shown to be specific, since no staining was observed on tissue that had been pretreated with heparinase enzymes (Fig. 1).

There is considerable diversity in the level and pattern of sulfation within HS GAG chains, which gives rise to a large repertoire of sequences that can be differentially recognized by different HS-binding proteins.[2,9,33] Phage-display antibodies have been developed that bind to specific HS structures,[12–15,23,24] providing tools to probe for differences in HS sulfation patterns within tissues.[20–22] In this study we used four such antibodies that recognize distinct HS epitopes (Table 1), where each produced a different binding pattern within the retina, choroid, and sclera (summarized in Table 2). As shown in Figures 2 and 3, all the HS antibodies bound strongly to the ILM, with the staining being particularly intense for LKIV69 (Table 2), which recognizes stretches of HS that are rich in *N*- and 2-*O*-sulfation but do not contain 6-*O*-sulfation. The RB4EA-12 antibody, which recognizes *N*- and 6-*O*-sulfation,[13,20–22] stained small focal patches in the GCL, and AO4B08, which binds to epitopes containing *N*-, 2- and 6-*O*-sulfation,[14] strongly labeled the NFL and retinal vasculature (Fig. 2B). The HS4C3 antibody, which recognizes primarily 3-*O*-sulfation in HS (Table 1), bound particularly well to GAG structures in the ILM (Figs. 3A, 3B) and in the vasculature of both the choroid (Fig. 3A) and neurosensory retina (Figs. 3B, 3C). Confocal microscopy of the latter allowed 3-D image reconstruction of HS4C3-positive blood vessels (e.g., running

Table 2. Intensity of Fluorescent Staining Demonstrated Using Particular Antibodies against Specific GAG Structures, Showing Differential Staining throughout the Layers of the Neurosensory Retina and Ocular Tissue

	Heparan Sulfate					Chondroitin Sulfate				Dermatan Sulfate	Hyaluronan	Keratan Sulfate
Tissue Layer	**10E4**	**LKIV69**	**RB4EA-12**	**AO4B08**	**HS4C3**	**1B5**	**2B6**	**3B3**	**LY111**	**286**	**bVG1**	**5D4**
Inner limiting membrane	+++	++++	+++	+++	++++	+++	+	++	+	++	++++	−
Nerve fiber layer	+++	+	+	+++	+	+++	++	++	++	++	+++	−
Ganglion cell layer	+++	+	+	+	+	++	++	++	+	++	++	−
Retinal blood vessels	++	+	+	+++	+++	++	++	++	++	++	++	−
Inner plexiform layer	++	+	+	++	+	++	+	++	++	++	++	−
Inner nuclear layer	++	+	+	++	+	++	+	++	+	++	++	−
Outer plexiform layer	++	+	+	++	+	+++	+	++	+	++	+++	−
Outer nuclear layer	++	+	+	+	+	++	+	++	+	++	++	−
Interphoto-receptor matrix	++	+	+	+	+	++++	+	+++	++	++	++	−
Retinal pigment epithelium	+++	+++	+++	+++	+++	+	+	++	++	++	+++	−
Bruch's membrane	+++	+	+++	+++	+++	+	+	+	+	++	++	−
Choroidal stroma	++	+	++	++	++	++	+++	++	++	++	+++	−
Choroidal blood vessels*	++	++	+++	+++	+++	+++	+	++++	+	++++	++++	−
Sclera	++	+++	++	++	++	+++	++	+++	++++	++++	++++	+++

Names of detection reagents used in this study are listed underneath their respective GAG class. The intensity of staining are classified as: −, absent; +, weak; ++, moderate; +++, strong; ++++, highly intense.

* Staining of large choroidal blood vessels was variable and the scores indicate intensity for most strongly labeled vessels.

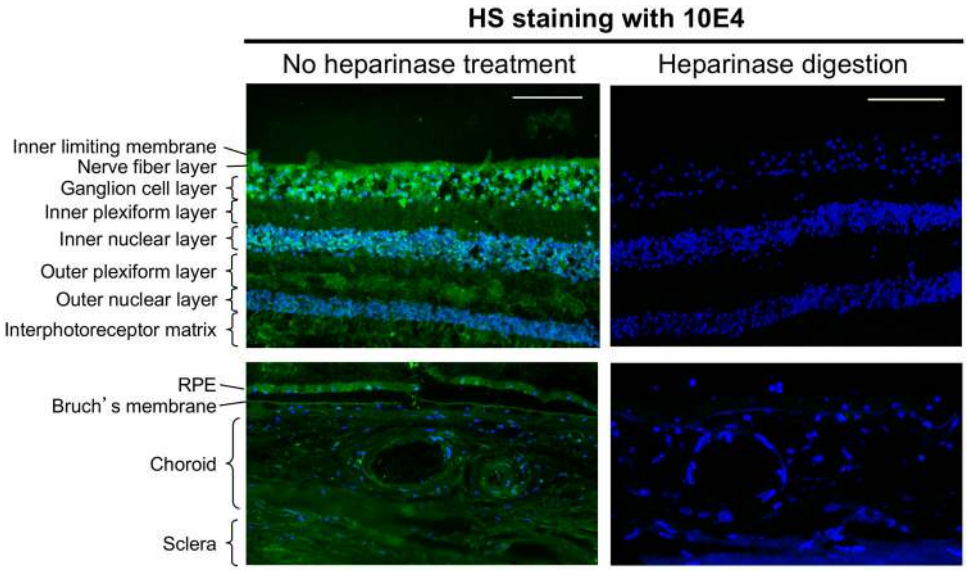

FIGURE 1. Localization of HS in retina, choroid, and sclera. Human tissue sections were stained using the pan HS antibody 10E4 (*green*) either without enzymatic pretreatment (*left side*) or after treatment with heparinases (*right side*). *Top*: the neurosensory retina; *bottom*: RPE, Bruch's membrane, choroid, and sclera. Here, and in all other figures, the images shown are representative of three individual donors (summarized in Table 2). *Blue*: DAPI staining of cell nuclei. Scale bar, 100 μm.

just beneath and parallel to the ILM; Fig. 3C). The phage-display antibodies also detected HS strongly in the retinal pigment epithelium (RPE), Bruch's membrane, and choroid (with the exception of LKIV69, which bound the latter two regions weakly). Thus, this panel of antibodies highlights the unique patterns of HS sulfation in different layers of the neurosensory retina, choroid, and sclera (Table 2).

Distribution of CS/DS and KS

The anti-stub antibodies used in this study recognize particular sulfation patterns in the residual GAG chain(s) left on CS/DS PGs after digestion with either chondroitin AC lyase or chondroitin B lyase.[16] The sulfation composition of the resulting CS/DS stub, still attached to the core protein, is believed to be representative of the sulfation pattern for the whole GAG chain.[16,34] For all the anti-stub antibodies used (Table 1), there was no staining in the absence of enzymatic pretreatment (data no shown), indicating that the detection after chondroitinase digestion was specific. After treatment with chondroitin AC lyase the antibody 3B3, which recognizes C6S stubs,[16] showed labeling throughout the retina, but this was particularly strong in the interphotoreceptor matrix (IPM; Fig. 4A). The 2B6 antibody, which recognizes C4S stubs,[16] generally produced low-level labeling throughout the retina, apart from labeling of the NFL, GCL, and retinal vasculature, which was moderate (Fig. 4A; Table 2). Interestingly, when we compared the 2B6 staining with the LY111 antibody, which was raised against the whole C4S GAG chain[17] (i.e., in the absence of any enzymatic pretreatment), we observed a similar overall pattern but with more intense fluorescence at both the IPM and sclera (Fig 4B); although pretreatment with chondroitin AC lyase abolished the majority of the signal with LY111, a small amount of residual

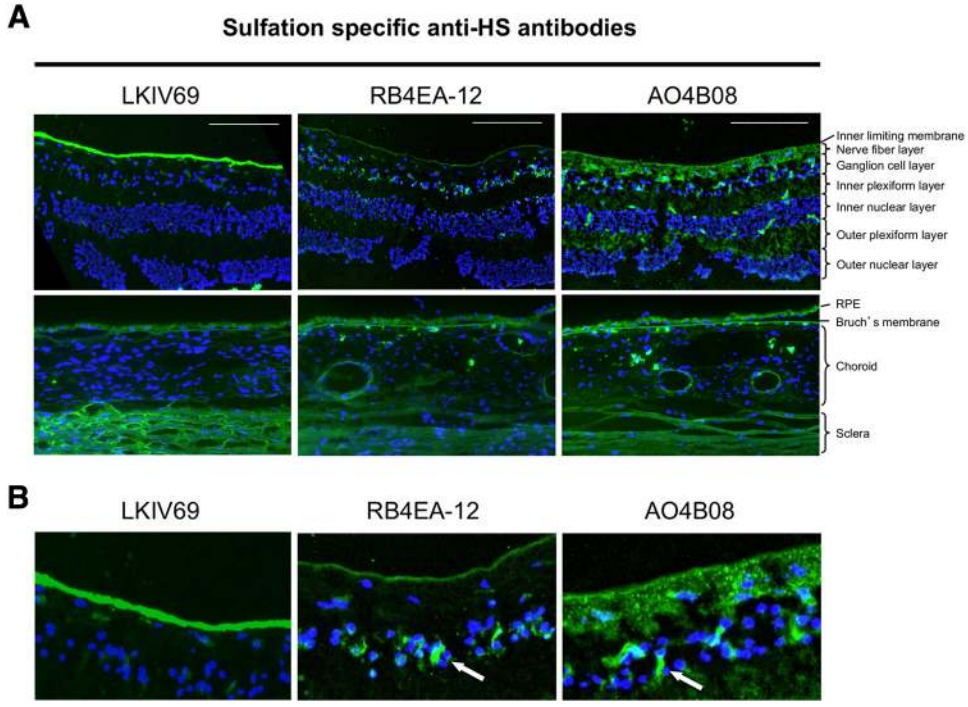

FIGURE 2. Detection of HS with sulfate-specific antibodies. Phage-display antibodies (Table 1) were used to map HS epitopes in the sclera and chorioretinal complex in human eye tissues (*green*). (**A**, *left*) LKIV69 recognizes *N*- and 2-*O*-sulfated regions of HS GAG chains; (*middle*) RB4EA-12 binds to sequences comprising iduronic acid followed by a glucosamine sulfated at the *N*- and 6-*O* positions; (*right*) AO4B08 recognizes *N*-sulfated octa-saccharide epitopes with three consecutive 6-*O* sulfates and an internal 2-*O* sulfate. (**B**) Close-up images of HS antibody staining in the inner retina; *arrows*: staining of retinal blood vessels with the RB4EA-12 and AO4B08 antibodies. Scale bar, 100 μm.

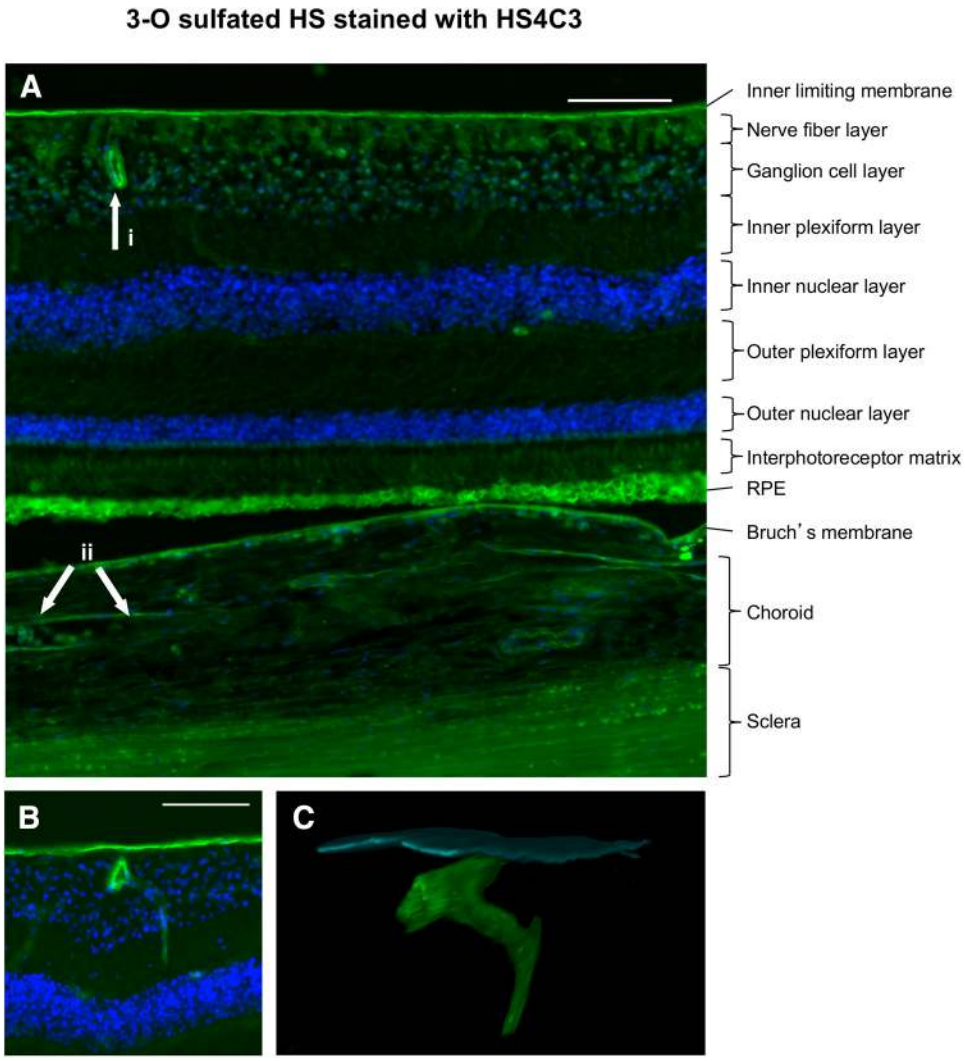

FIGURE 3. Distribution of 3-*O*-sulfated HS epitopes in retina and choroid. (**A**) Staining of retina and choroid with HS4C3 (*green*), which recognizes 3-*O*-sulfated HS containing the antithrombin binding sequence (see Table 1); *arrows*: blood vessels in the retina (i) and choroid (ii), which stain strongly with this antibody. (**B**) Detail of a retinal blood vessel (from the same donor) lying underneath the ILM (scale bar, 50 μm). (**C**) Three-dimensional reconstruction by confocal microscopy of blood vessel in (**B**) in which the ILM is pseudocolored *blue* for clarity. Scale bar: (**A**, **C**) 100 μm; (**B**) 50 μm.

staining was observed in the RPE and sclera. Interestingly, the 1B5 antibody, which recognizes unsulfated CS stubs (Table 1), gave rise to strong labeling throughout the retina that was particularly intense in the ILM, NFL, outer plexiform layer (OPL), and IPM (Table 2). Some choroidal blood vessels were found to contain unsulfated CS (strong 1B5 staining) and 6-*O*-sulfated CS (very strong 3B3 staining), but there was much less labeling with the antibodies to C4S (2B6 and LY111; Fig. 4A).

The 2B6 antibody can also recognize stubs of DS after digestion with the DS-specific enzyme chondroitin B lyase[18]; using this approach we observed moderate DS staining throughout the retina (Fig. 5 top; Table 2). There was, however, intense staining in the walls of some choroidal blood vessels and in the sclera (Fig. 5, bottom).

The 5D4 antibody, which recognizes a wide range of structures in the whole KS chain,[19] was used to visualize this GAG in the human eye tissue sections. KS was not detected in either the retina or the choroid, but the sclera was labeled strongly (Fig. 6).

Distribution of HA

HA, which is ubiquitously present in all vertebrates, has an identical structure, regardless of the species/tissue that produces it,[6] thus making it inherently difficult to raise specific, high titer, antibodies against this GAG. Therefore, it is common to employ an HA-binding protein as a probe for the localization of HA in tissue sections. Here we have made a novel HA-detection reagent by biotinylating a recombinant G1 domain of versican (bVG1); this was expressed in *E. coli*, refolded, and purified (Figs. 7A–C), and shown to interact with HA via a solid-phase binding assay (Fig. 7D).

Labeling of tissue sections with bVG1 was shown to be specific for HA by the complete removal of the fluorescent signal on tissue pretreatment with hyaluronidase, with the exception of a few individual cells, mainly within the choroid, that remained positive (Fig. 8B). Other control experiments demonstrated that the bVG1 used here gave a very similar staining pattern and specificity compared with another commercially available HA probe (bHABP; Figs. 8C, 8D). As can be seen from Figure 8A (and Table 2), staining with bVG1 revealed that HA was present throughout the retina and choroid, with particularly high levels observed in the walls of large retinal and choroidal blood vessels and associated with the RPE, especially on its apical surface (Fig. 8A, arrow). Intense staining was also present at the ILM but this may be as a result of labeling of cortical vitreous still associated with the section.

DISCUSSION

The multiple biological functions of GAGs, important to both their physiology and pathology, results largely from their abil-

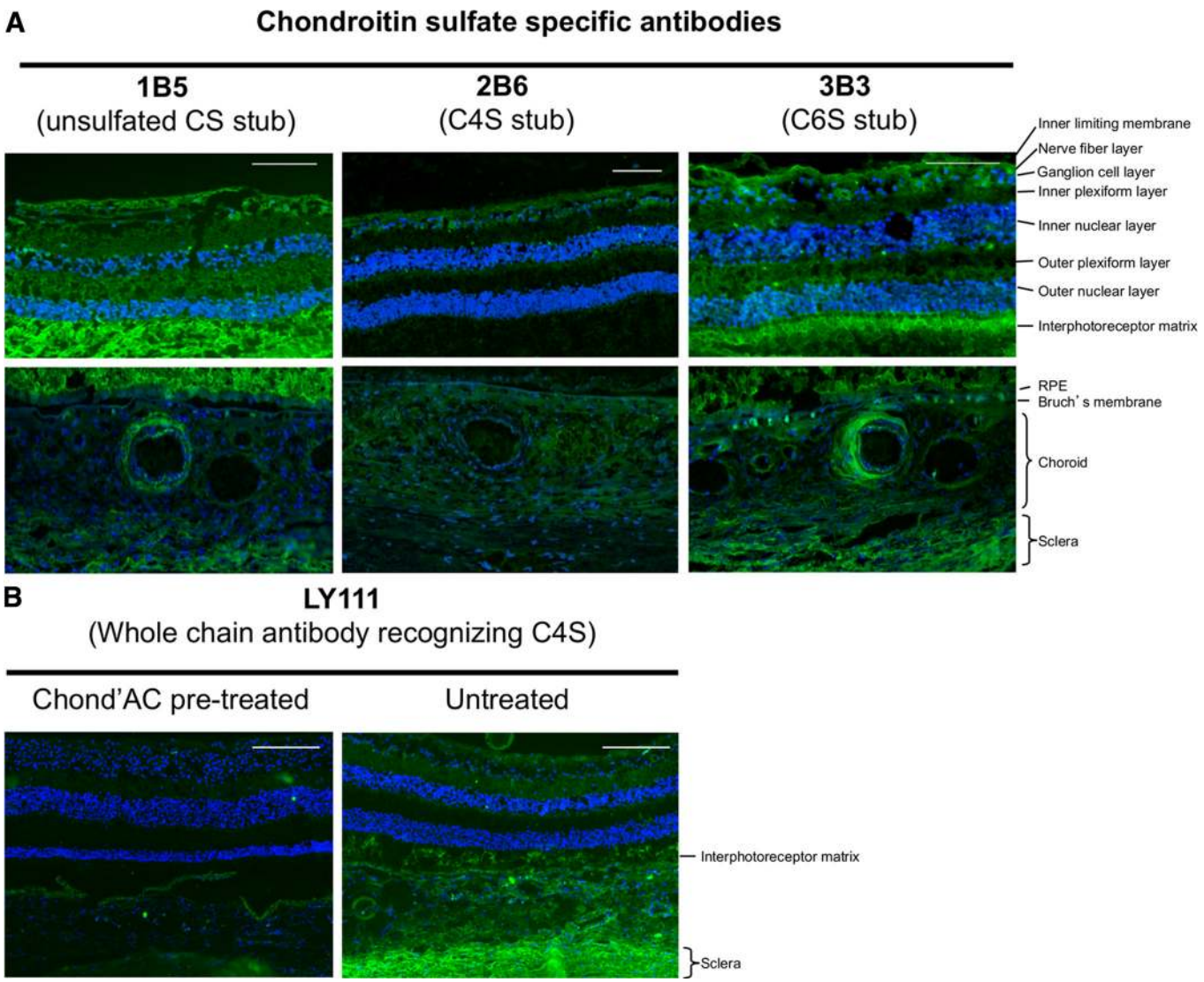

Figure 4. Localization of CS subtypes in retina, choroid, and sclera. The presence of CS was detected using either (**A**) anti-stub antibodies (1B5, 2B6, and 3B3; Table 1) after chondroitin AC lyase digestion or (**B**) the LY111 antibody raised against a whole C4S chain. *Top*: the neurosensory retina; *bottom*: the RPE, choroid, and sclera. (**B**) Digestion with chondroitin AC lyase removed ~90% of the *green* fluorescent signal associated with LY111, although some residual labeling of the RPE and sclera remains. Scale bar, 100 μm.

ity to interact with many different proteins including growth factors (e.g., VEGFs and FGFs), growth factor receptors, chemokines, matrix molecules, proteases, and enzyme inhibitors.[2,3] Therefore, to understand GAG-mediated regulation of protein function in the context of retinal cell biology and disease mechanisms (e.g., in AMD[9,35]), it is important to have a detailed understanding of which GAGs are present in the human eye along with their relative distribution. Here we have compiled a detailed map of CS, DS, HA, HS, and KS in the adult human retina, choroid, and sclera, revealing GAG-specific differences in their localization.

HS has been previously reported to be present in basement membrane–containing structures in the human retina, including the ILM, retinal vessel walls, and Bruch's membrane, on the basis of staining with cupromeronic blue[31] and anti-stub antibodies.[32] Although our data are consistent with these observations, we further identified HS in other parts of the choroidal–retinal complex: HS was present throughout the retina, including the nerve fiber layer, ganglion cell layer, and RPE. A similar widespread distribution of HSPGs has been observed in embryonic rat retinas.[8]

In this study we also used phage-display antibodies that label a restricted subset of HS structures. These antibodies revealed significant differences in the sulfation pattern of HS present within the various regions of the retina, choroid, and sclera.

For example, HS4C3, which recognizes the antithrombin binding sequence,[15] strongly stained the ILM and underlying blood vessels, revealing a high level of 3-*O* sulfation at the neurosensory retina–vitreous interface. The ILM also stained strongly with AO4B08 and RB4EA-12 (antibodies that can recognize epitopes containing 6-*O*-sulfation), whereas, LKIV69, the binding of which can be inhibited by 6-*O*-sulfation,[12,21] gave the most intense labeling of this region. This suggests that the ILM contains diverse HS structures, such that both the presence and absence of 6-*O*-sulfation could have implications for the binding and regulation of proangiogenic growth factors, such as VEGF and FGF2,[36,37] (i.e., to prevent aberrant blood vessel growth from the neurosensory retina into the vitreous).

Our observation that most of these anti-HS antibodies bound well to the Bruch's membrane in the adult human eye,

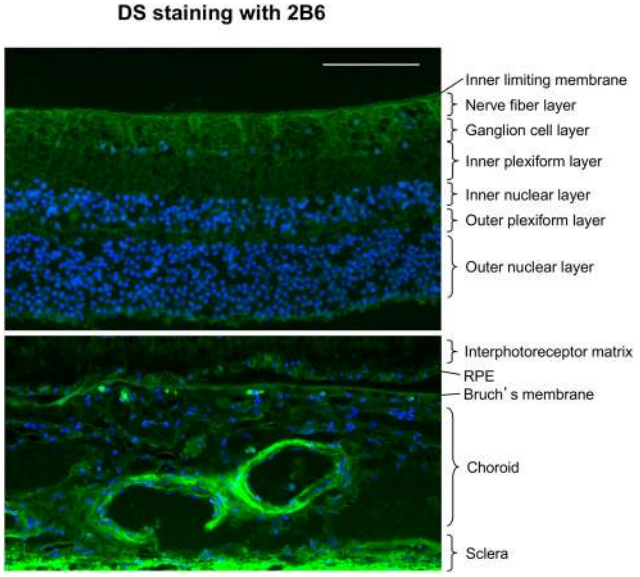

FIGURE 5. Distribution of DS determined with 2B6 antibody. DS stubs were detected with 2B6 antibody (*green*) after predigestion of sections with chondroitin B lyase. Scale bar, 100 μm.

indicates that there is a wide range of HS structures and motifs present within this extracellular matrix, containing *N*-, 6-*O*- and 2-*O*-sulfated regions (AO4B08/LKIV69), 3-*O*-sulfated structures (HS4C3), and HS with a lower level of 2-*O*-sulfation (RB4EA-12). Interestingly, we found previously that the 402H polymorphic variant of complement factor H, which is associated with

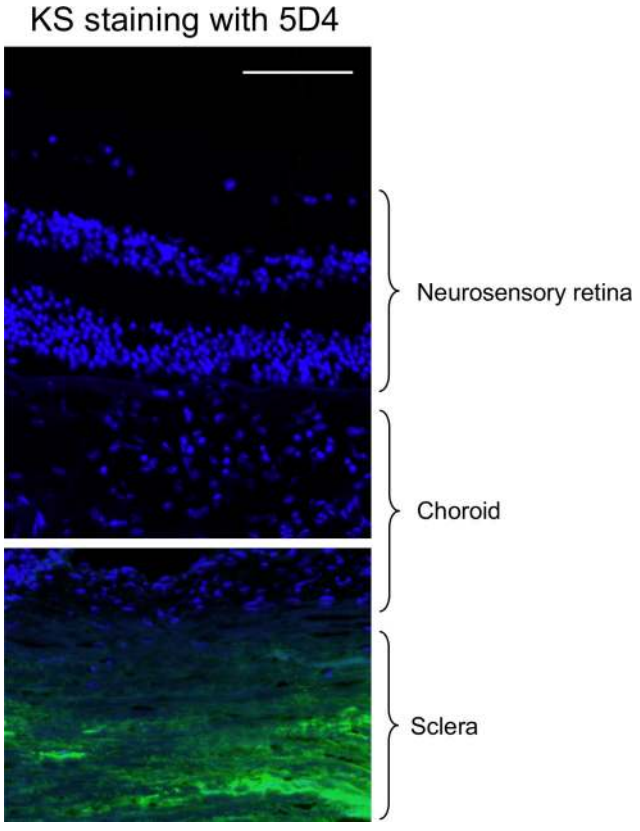

FIGURE 6. KS is present only in sclera of the adult human eye. KS GAG chains (*green*) were detected with the pan-specific antibody 5D4. Scale bar, 100 μm.

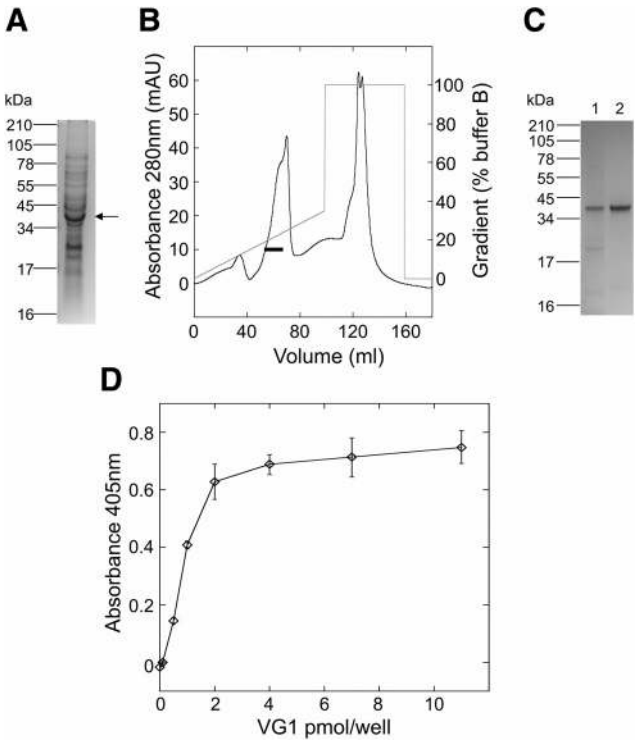

FIGURE 7. Expression, purification, and HA-binding activity of VG1. (**A**) Protein expression was induced with IPTG and cultures analyzed after 20 hours by SDS-PAGE (under reducing conditions), revealing a band at ~40 kDa (*arrow*) that had the expected N-terminal sequence (data not shown). (**B**) After inclusion body preparation and refolding, VG1 was purified by ion exchange chromatography (Q Sepharose); *horizontal bar*: pooled eluents. (**C**) The VG1 preparation was analyzed by SDS-PAGE after refolding (*lane 1*) and ion exchange chromatography (*lane 2*), revealing the purity of the recombinant protein. (**D**) The HA-binding activity of the VG1 was demonstrated using biotinylated-HA binding to VG1 immobilized on microtiter plates at a range of concentrations (0–11 pmol/well). Values are plotted as the mean absorbance (A_{405nm}) ±SE ($n = 8$).

AMD, requires 2-*O*- and/or 6-*O*-sulfation for its binding to HS in human Bruch's membrane,[10] whereas the 402Y form (non–disease-associated) likely has a broader GAG specificity.[28] Thus, based on the data described herein, it is possible that there is a smaller number of HS sequences capable of supporting 402H binding to Bruch's membrane (compared to 402Y). This may explain, at least in part, the lower level of the AMD-associated form of complement factor H seen to bind to this extracellular matrix in our recent study.[10] Importantly, poor binding of the 402H variant to Bruch's membrane may provide a potential disease mechanism for AMD.[9,10,35]

A previous study using the same anti-CS/DS stub antibodies as were used in the present study found strong labeling of the human IPM and sclera with 3B3 (specific for 6-sulfated CS stubs), but did not observe any staining with either 1B5 or 2B6[38]; the CSPG SPACRCAN was subsequently identified in the IPM.[39] However, in addition to the labeling of the IPM/sclera with 3B3, we saw immunoreactivity for this antibody throughout the retina and choroid. Moreover, we observed strong labeling of the IPM with the 1B5 antibody (recognizing unsulfated CS stubs), as well as other regions of the retina, including the ILM. The staining we observed with 2B6 (4-sulfated CS stubs) (e.g., in the choroidal stroma and NFL), was largely consistent with the pattern seen with the anti-C4S whole-chain antibody LY111 (Fig. 4). The more intense staining of the IPM and sclera with the latter, likely results from the greater num-

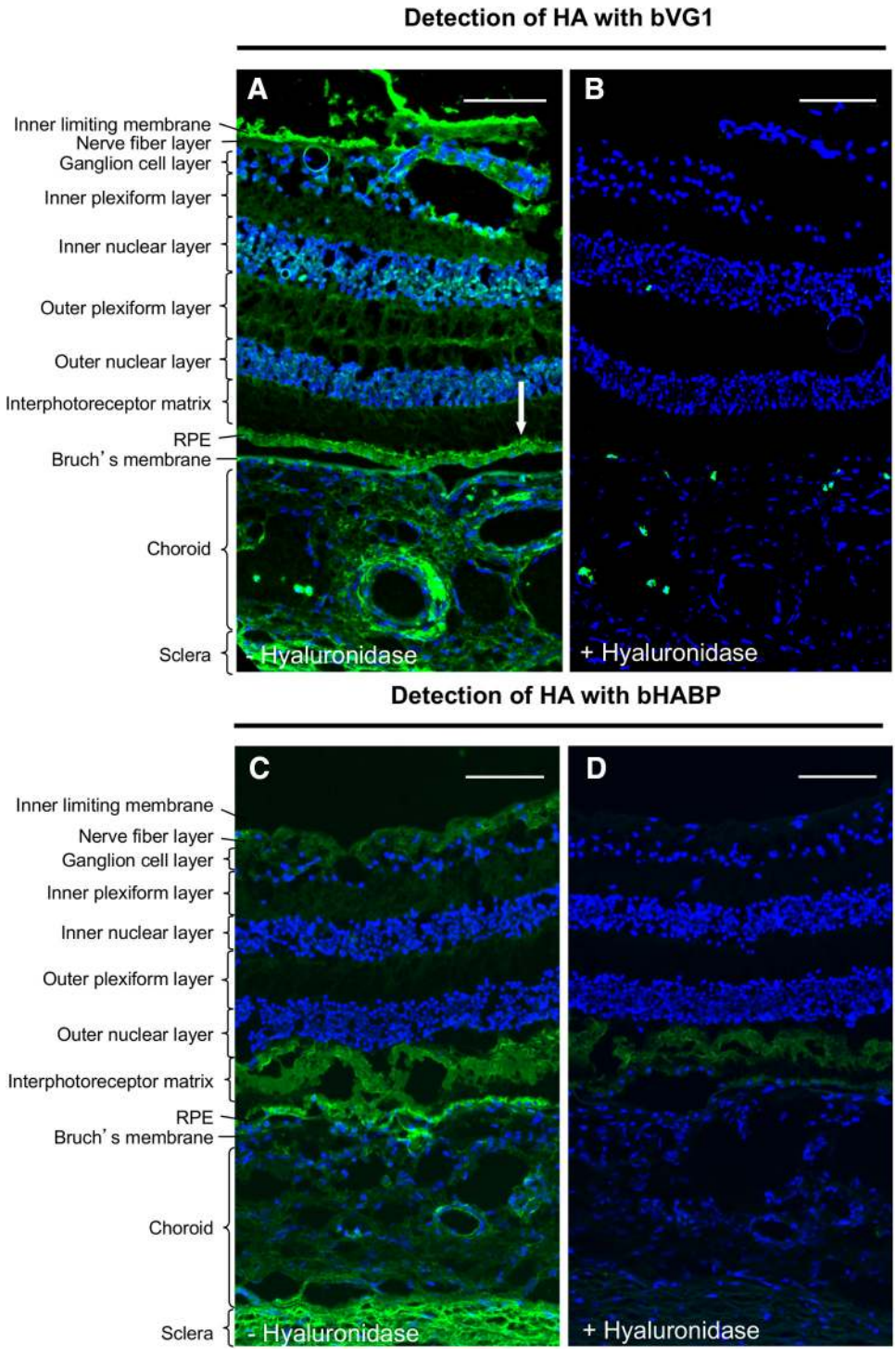

FIGURE 8. Localization of HA in the retina and choroid. HA (*green*) was detected with our bVG1 (*top*) and a commercially available HA-binding protein (bHABP; *bottom*) in the absence (**A**, **C**) and presence (**B**, **D**) of hyaluronidase pretreatment. (**A**) Strong labeling was seen, for example, in choroidal blood vessels and on the RPE, with intense staining on its apical side (*arrow*). (**B**) The staining of a few individual cells remaining after hyaluronidase digestion, which are mostly in the lumen of blood vessels, probably resulted from the interaction of the VG1 protein with other versican ligands. (**C**) A similar pattern of HA localization was observed with bHABP, except that the staining seen in the IPM is likely to be nonspecific, given that it was not fully removed by hyaluronidase treatment (**D**). Scale bar, 100 μm.

ber epitopes for LY111 on whole C4S GAG chains, as opposed to the individual stubs generated by chondroitinase AC digestion. Here we used frozen sections of tissue lightly fixed with formaldehyde, rather than paraffin embedding of tissue after fixation with glutaraldehyde/formaldehyde,[38] which may explain the difference in the staining patterns seen in these two studies.

While DS has been described previously in Bruch's membrane,[31] this, to our knowledge, is the first time that it has been shown to be widely distributed in the human retina and choroid (e.g., with intense staining seen in choroidal blood vessels), although CS and DS GAGs have been reported in association with collagen fibrils in the human sclera.[40,41] This result also supports our recent findings that the binding of complement factor H to Bruch's membrane and RPE can be significantly reduced by treatment with chondroitin B lyase, indicating that it interacts with DS in these locations.[10]

We determined the distribution of HA using a novel detection reagent, bVG1. Another study using a similar probe (comprising the HA-binding region of aggrecan and link protein, both of which are homologues of versican[42]) detected HA in the IPM, ILM, and, to a lesser extent, in the NFL and plexiform layers of the retina.[43] Although this finding is in agreement with our data, we also observed strong labeling throughout the

retina and choroid. The intense staining of HA on the apical surface of the RPE (Fig. 8) perhaps indicates that this GAG has a role in the attachment of the IPM (and thus the retina) to the RPE particularly as the IPM has been shown to contain the HA-binding CSPG SPACRCAN.[39]

We did not observe any KS in either the retina or choroid; however, we saw intense staining in the sclera. The antibody used recognizes a wide range of KS sulfation patterns.[19] While we cannot rule out that KS species not detected by this antibody are present in the retina and choroid, our finding is consistent with the absence of retinal KS reported previously in the rat eye.[44] Interestingly, transient expression of the KSPG claustrin has been seen in the developing chick embryo,[45] where it was downregulated after embryonic day 17.[46] Therefore, in humans it remains possible that KS is transiently expressed in the retinal–choroidal complex during development.

In conclusion, this study provides a detailed reference map of the distribution of GAGs in the adult human retina, choroid, and sclera. This will greatly assist future research aimed at understanding the role of GAG-protein interactions and their regulation in both physiological and pathologic processes.

Acknowledgments

The authors thank Isaac Zambrano (Corneal Transplant Service, Manchester Eye Bank, Manchester Royal Eye Hospital) for supplying the donor eye tissue, Simon J. Foulcer for assistance with preparation of the VG1 protein (University of Manchester), Tony Willis for the N-terminal sequencing of recombinantly expressed VG1 (University of Oxford), and Jane Kott for help with the microscopy.

References

1. Theocharis AD, Skandalis SS, Tzanakakis GN, Karamanos NK. Proteoglycans in health and disease: novel roles for proteoglycans in malignancy and their pharmacological targeting. *FEBS Lett J.* 2010; 277:3904–3923.
2. Lindahl U, Li JP. Interactions between heparan sulfate and proteins-design and functional implications. *Int Rev Cell Mol Biol.* 2009;276:105–159.
3. Kresse H, Schonherr E. Proteoglycans of the extracellular matrix and growth control. *J Cell Physiol.* 2001;189:266–274.
4. Taylor KR, Gallo RL. Glycosaminoglycans and their proteoglycans: host-associated molecular patterns for initiation and modulation of inflammation. *FASEB J.* 2006;20:9–22.
5. Mulloy B, Forster MJ. Conformation and dynamics of heparin and heparan sulfate. *Glycobiology.* 2000;10:1147–1156.
6. Tammi MI, Day AJ, Turley EA. Hyaluronan and homeostasis: a balancing act. *J Biol Chem.* 2002;277:4581–4584.
7. Toole BP. Hyaluronan: from extracellular glue to pericellular cue. *Nat Rev Cancer.* 2004;4:528–539.
8. Inatani M, Tanihara H. Proteoglycans in retina. *Prog Retin Eye Res.* 2002;21:429–447.
9. Clark SJ, Bishop PN, Day AJ. Complement factor H and age-related macular degeneration: the role of glycosaminoglycan recognition in disease pathology. *Biochem Soc Trans.* 2010;38:1342–1348.
10. Clark SJ, Perveen R, Hakobyan S, et al. Impaired binding of the age-related macular degeneration-associated complement factor H 402H allotype to Bruch's membrane in human retina. *J Biol Chem.* 2010;285:30192–30202.
11. David G, Bai XM, van der Schueren B, Cassiman JJ, van den Berghe H. Developmental changes in heparan sulfate expression: In situ detection with mAbs. *J Cell Biol.* 1992;119:961–975.
12. Wijnhoven TJ, de Westerlo EM, Smits NC et al. Characterization of anticoagulant heparinoids by immunoprofiling. *Glycoconj J.* 2008; 25:177–185.
13. Dennissen MABA, Jenniskens GJ, Pieffers M, et al. Large, tissue-regulated domain diversity of heparan sulfates demonstrated by phage display antibodies. *J Biol Chem.* 2002;277:10982–10986.
14. Kurup S, Wijnhoven TJM, Jenniskens GJ et al. Characterization of anti-heparan sulfate phage display antibodies AO4B08 and HS4E4. *J Biol Chem.* 2007;282:21032–21042.
15. ten Dam GB, Kurup S, van de Westerlo EMA, et al. 3-O-sulfated oligosaccharide structures are recognized by anti-heparan sulfate antibody HS4C3. *J Biol Chem.* 2006;281:4654–4662.
16. Caterson B, Christner JE, Couchman JR. Production and characterization of monoclonal antibodies directed against connective tissue proteoglycans. *Fed Proc.* 1985;44:386–393.
17. Yada T, Arai M, Suzuki S, Kimata K. Occurrence of collagen and proteoglycan forms of type IX collagen in chick embryo cartilage. *J Biol Chem.* 1992;267:9391–9397.
18. Jandik KA, Gu K, Linhardt JL. Action pattern of polysaccharide lyases on glycosaminoglycans. *Glycobiology.* 1994;4:289–296.
19. Caterson B, Christner JE, Barker JR. Identification of a monoclonal antibody that specifically recognizes corneal and skeletal keratan sulfate: monoclonal antibodies to cartilage proteoglycans. *J Biol Chem.* 1983;258:8848–8854.
20. Lamanna WC, Baldwin RJ, Padva M, et al. Heparan sulphate 6-O-endosulphatases-discrete in vivo activities and functional cooperativity. *Biochem J.* 2006;400:63–73.
21. Johnson CE, Crawford BE, Stavridis M, et al. Essential alterations of heparan sulfate during the differentiation of embryonic stem cells to Sox1-enhanced green fluorescent protein-expressing neural progenitor cells. *Stem Cells.* 2007;25:1913–1923.
22. Baldwin RB, ten Dam GB, van Kuppevelt TH, et al. A developmentally-regulated heparan sulfate epitope defines a sub-population with increased blood potential during mesodermal differentiation. *Stem Cells.* 2008;26:3108–3118.
23. Van Kuppevelt TH, Dennissen MABA, van Venrooij WJ, Hoet RMA, Veerkamp JH. Generation and application of type-specific anti-heparan sulfate antibodies using phage display technology. *J Biol Chem.* 1998;273:12960–12966.
24. Jenniskens GJ, Oosterhof A, Brandwijk R, Veerkamp JH, van Kuppevelt TH. Heparan sulfate heterogeneity in skeletal muscle basal lamina: demonstration by phage display-derived antibodies. *J Neurosci.* 2000;20:4099–4111.
25. Zimmermann DR, Ruoslahti E. Multiple domains of the large fibroblast proteoglycan, versican. *EMBO J.* 1989;8:2975–2981.
26. Seyfried NT, McVey GF, Almond A, et al. Expression and purification of functionally active hyaluronan-binding domains from human cartilage link protein, aggrecan and versican: formation of ternary complexes with defined hyaluronan oligosaccharides. *J Biol Chem.* 2005;280:5435–5448.
27. Day AJ, Aplin RT, Willis AC. Overexpression, purification, and refolding of link module from human TSG-6 in Escherichia coli: effect of temperature, media, and mutagenesis on lysine misincorporation at arginine AGA codons. *Protein Expr Purif.* 1996;8:1–16.
28. Clark SJ, Higman VA, Mulloy B, et al. His-384 allotypic variant of factor H associated with age-related macular degeneration has different heparin binding properties from the non-disease-associated form. *J Biol Chem.* 2006;281:24713–24720.
29. White J, Lukacik P, Esser D, et al. Biological activity, membrane-targeting modification, and crystallization of soluble human decay accelerating factor expressed in E. coli. *Protein Sci.* 2004;13:2406–2415.
30. Kuznetsova SA, Issa P, Perruccio EM, et al. Versican-thrombospondin-1 binding in vitro and colocalization in microfibrils by inflammation on vascular smooth muscle cells. *J Cell Sci.* 2006;119:4499–4509.
31. Call TW, Hollyfield JG. Sulfated proteoglycans in Bruch's membrane of the human eye: localization and characterization using cupromeronic blue. Exp. *Eye Res.* 1990;51:451–462.
32. Witmer AN, van den Born J, Vrensen GFJM and Schlingemann RO. Vascular localization of heparan sulfate proteoglycans in retinas of patients with diabetes mellitus and in VEGF-induced retinopathy using domain-specific antibodies. *Curr Eye Res.* 2001;3:190–197.
33. Esko JD, Selleck SB. Order out of chaos: assembly of ligand binding sites in heparan sulfate. *Annu Rev Biochem.* 2002;71:435–471.
34. Couchman JR, Caterson B, Christner JE, Baker JR. Mapping by monoclonal antibody detection of glycosaminoglycans in connective tissues. *Nature.* 1984;307:650–652.
35. Day AJ, Clark SJ, Bishop PN. Understanding the molecular basis of age-related macular degeneration and how the identification of

new mechanisms may aid the development of novel therapies. *Expert Rev Ophthalmol.* 2011;6:123–128.

36. Ashikari-Hada S, Habuchi H, Kariya Y, Kimata K. Heparin regulates vascular endothelial growth factor165-dependent mitotic activity, tube formation, and its receptor phosphorylation of human endothelial cells. *J Biol Chem.* 2005;280:31508–31515.
37. Fuster MM, Wang L. Endothelial heparan sulfate in angiogenesis. *Prog Mol Biol Transl Sci.* 2010;93:179–212.
38. Hollyfield JG, Rayborn ME, Midura RJ, Shadreach KG, Acharya S. Chondroitin sulfate proteoglycan core proteins in the interphotoreceptor matrix: a comparative study using biochemical and immunohistochemical analysis. *Exp Eye Res.* 1999;69:311–322.
39. Acharya S, Foletta VC, Lee JW et al. SPACRCAN, a novel human interphotoreceptor matrix hyaluronan-binding proteoglycan synthesized by photoreceptors and pinealocytes. *J Biol Chem.* 2000; 275:6945–6955.
40. Young RD. The ultrastructural organization of proteoglycans and collagen in human and rabbit scleral matrix. *J Cell Sci.* 1985;74: 95–104.
41. Quantock AJ, Mek KM. Axial electron density of human scleral collagen: Location of proteoglycans by X-ray diffraction. *J Biophys.* 1988;54:159–164.
42. Day AJ, Prestwich GD. Hyaluronan-binding proteins: tying up the giant. *J Biol Chem.* 2002;277:4585–4588.
43. Hollyfield JG, Rayborn ME, Tammi M, Tammi R. Hyaluronan in the interphotoreceptor matrix of the eye: species differences in content, distribution, ligand binding and degradation. *Exp Eye Res.* 1998;66:241–248.
44. Geisert EE, Williams RC, Bidanset DJ. A CNS specific proteoglycan associated with astrocytes in rat optic nerve. *Brain Res.* 1992;571: 165–168.
45. McAdams BD, McLoon SC. Expression of chondroitin sulfate and keratan sulfate proteoglycans in the path of growing retinal axons in the developing chick. *J Comp Neurol.* 1995;352:594–606.
46. McCabe CF, Cole GJ. Expression of the barrier-associated proteins EAP-300 and claustrin in the developing central nervous system. *Brain Res Dev Brain Res.* 1992;70:9–24.